

Affinity of the Highly Preorganized Ligand PDA (1,10-Phenanthroline-2,9-dicarboxylic acid) for Large Metal Ions of Higher Charge. A Crystallographic and Thermodynamic Study of PDA Complexes of Thorium(IV) and the Uranyl(VI) ion

Nolan E. Dean,[†] Robert D. Hancock,^{*,‡} Christopher L. Cahill,^{*,‡} and Mark Frisch[‡]

Department of Chemistry and Biochemistry, University of North Carolina–Wilmington, Wilmington, North Carolina 28403, and Department of Chemistry, George Washington University, Washington, D.C. 20052

Received August 7, 2007

The hydrothermal synthesis and structures of $[\text{UO}_2(\text{PDA})]$ (**1**) and $[\text{Th}(\text{PDA})_2(\text{H}_2\text{O})_2] \cdot \text{H}_2\text{O}$ (**2**) (PDA = 1,10-phenanthroline-2,9-dicarboxylic acid) are reported. **1** is orthorhombic, $Pnma$, $a = 11.1318(7) \text{ \AA}$, $b = 6.6926(4) \text{ \AA}$, $c = 17.3114(12) \text{ \AA}$, $V = 1289.71(14)$, $Z = 4$, $R = 0.0313$; **2** is triclinic, $P\bar{1}$, $a = 7.6190(15) \text{ \AA}$, $b = 10.423(2) \text{ \AA}$, $c = 17.367(4) \text{ \AA}$, $\alpha = 94.93(3)^\circ$, $\beta = 97.57(3)^\circ$, $\gamma = 109.26(3)^\circ$, $V = 1278.3(4) \text{ \AA}^3$, $Z = 2$, $R = 0.0654$. The local geometry around the U in **1** is a pentagonal bipyramid with the two uranyl oxygens occupying the apical positions. The donor atoms in the plane comprise the four donor atoms from the PDA ligand (average U–N = 2.558 and U–O = 2.351 \AA) with the fifth site occupied by a bridging carboxylate oxygen from a neighboring UO_2/PDA individual. The PDA ligand in **1** is exactly planar, with the U lying in the plane of the ligand. The latter planarity, as well as the near-ideal U–O and U–N bond lengths, and O–U–N and N–U–N bond angles within the chelate rings of **1** suggest that PDA binds to the uranyl cation in a low-strain manner. In **2**, there are two PDA ligands bound to the Th (average Th–N = 2.694 and Th–O = 2.430 \AA) as well as two water molecules (Th–O = 2.473 and 2.532 \AA) to give the Th a coordination number of 10. The PDA ligands in **2** are bowed, with the Th lying out of the plane of the ligand. Molecular mechanics calculations suggest that the distortion of the PDA ligands in **2** arises because of steric crowding. UV spectroscopic studies of solutions containing 1:1 ratios of PDA and Th^{4+} in 0.1 M NaClO_4 at 25 $^\circ\text{C}$ indicate that $\log K_1$ for the $\text{Th}^{4+}/\text{PDA}$ complex is 25.7(9). The latter result confirms the previous prediction that complexes of PDA with metal ions of higher charge and an ionic radius of about 1.0 \AA such as Th(IV) would have remarkably high $\log K_1$ values with PDA. The origins of this very high stability are discussed in terms of a synergy between the pyridyl and the carboxylate donor groups of PDA. Metal ions of high charge normally bond poorly with pyridyl donors in aqueous solution because such metal ions require donor groups that are able to disperse charge to the solvent via hydrogen-bonding, which pyridyl groups are unable to do. In PDA, the carboxylates fulfill this need and so enable the high donor strength of the pyridyl groups of PDA to become apparent in the high $\log K_1$ for Th(IV) with PDA.

Introduction

The selective complexation of the minor actinides Am(III) and Cm(III) in the presence of Ln(III) (Ln = Lanthanide)

ions in reprocessing of spent nuclear fuel is currently of importance.¹ Lanthanides such as Gd, Sm, and Eu have large neutron-capture cross-sections, so that further treatment of recovered minor actinides in nuclear reactors is inhibited by

* To whom correspondence should be addressed. E-mail: hancockr@uncw.edu (R.D.H.); cahill@gwu.edu (C.L.C.).

[†] University of North Carolina–Wilmington.

[‡] George Washington University.

(1) Nash, K. L.; Madic, C.; Mathur, J. N.; Lacquement, J. In *The Chemistry of the Actinide and Transactinide Elements*, 3rd ed.; Morss, L. R., Edelstein, N. M., Fuger, J., Eds.; Springer: Dordrecht, The Netherlands, 2006, Vol. 4, p 2622.

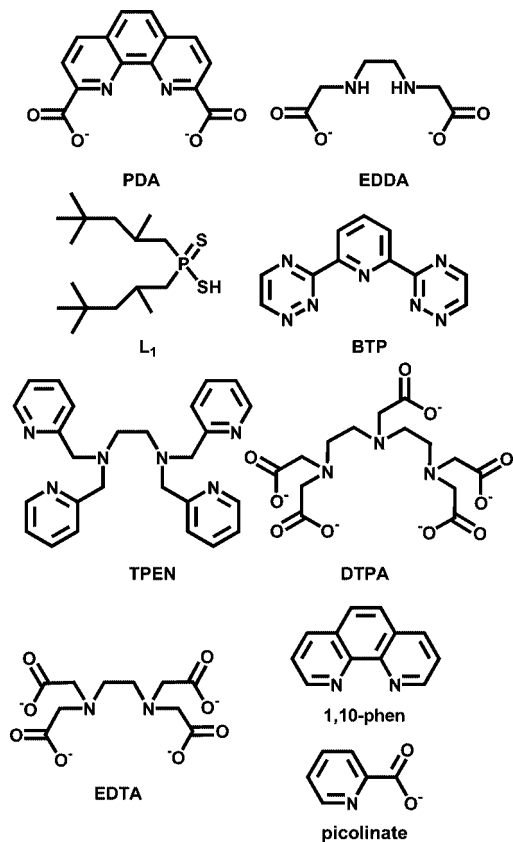
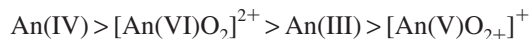


Figure 1. Ligands discussed in this paper.

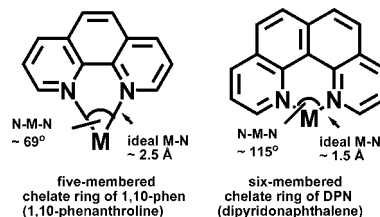
the presence of these Ln(III) ions. The complexing strengths of actinides (An) with ligands tend to vary² as



One can thus exploit the greater affinity for ligands shown by major actinides such as U, Np, and Pu that can more easily attain the An(IV) or $[\text{An(VI)O}_2]^{2+}$ state to separate these from Ln(III) ions. However, for Am and Cm, one is reaching the later part of the actinide series, where the elements are coming to resemble Ln(III) ions in that higher oxidation states are attained with greater difficulty, and the An(III) state is dominant. It therefore seems possible that, at least with ligand types studied to date, any separation of Am and Cm from Ln ions will have to rely on differences in chemistry between the An(III) and Ln(III) ions. These two groups of ions are similar in ionic radius³ and coordination number, so that size differences are not promising as an approach to effect separations. The most important difference was first recognized by Seaborg,⁴ who noted that An cations appeared to be more covalent in their bonding than their Ln counterparts. This difference in covalency forms the basis of current proposed separations of An(III) ions from Ln(III) ions.⁵ Ligands used to selectively complex Am(III) rely on the presence of donor groups softer than oxygen,

such as nitrogen-donors (N-donors) and sulfur-donors (S-donors). Thus, for example, Tian et al.⁶ have used the S-donor ligand L1 in Figure 1 to achieve selectivity for Am(III) over Eu(III) of 1×10^3 . Aromatic N-donor ligands such as BTP (Figure 1) appear⁷ to be promising for such separations, with the added advantage of greater resistance to decomposition than S-donor ligands. It has been shown⁸ that pyridine-containing N-donor ligands such as TPEN (Figure 1) have selectivities for Am(III) over Ln(III) ions of about 1×10^2 .

In a recent paper,⁹ some metal ion complexing properties of the ligand PDA (Figure 1) were reported. PDA has high levels of preorganization¹⁰ because of the rigidity provided by the aromatic backbone, which leads to remarkably high $\log K_1$ values for a tetradentate ligand. Thus, at neutral pH, PDA can displace the octadentate DTPA from its Gd(III) complex. PDA also has a high affinity for metal ions with an ionic radius close to 1.0 Å. This can be understood⁹ in terms of the idea that PDA has a rigid “cleft” that forms three 5-membered chelate rings, which favor^{9,11,12} larger metal ions. In contrast 6-membered rings favor small metal ions, for simple geometric reasons indicated in the following graphic: PDA is of interest because of its possession of



aromatic N-donors, rather like BTP, which appears⁷ to be currently of the type of most promising N-donor ligand for the selective complexation of actinides. What was significant in the chemistry of PDA was the very rapid increase in $\log K_1$ with metal ions, all of ionic radius³ (r^+) about 1.0 Å, but of increasing charge. It should be noted that these are effective ionic radii that for cations are 0.14 Å smaller than crystal ionic radii. Thus, for Ca(II) ($r^+ = 1.00$ Å),³ $\log K_1(\text{PDA}) = 7.3$, but with Gd(III) ($r^+ = 0.96$ Å), $\log K_1(\text{PDA}) = 16.1$. This can be contrasted with the much smaller difference in $\log K_1$ that occurs⁹ with EDDA¹³ ($\log K_1$ Ca(II) = 4.0, Gd(III) = 8.1), the much less preorganized analog of PDA. The dependence of the affinity of metal ions for PDA on their charge, as indicated by extrapolation from $\log K_1(\text{PDA})$ for Ca(II) to Gd(III), suggests that $\log K_1$ with the actinide Th(IV) should be extremely high. Of relevance also is the affinity of PDA for the UO_2^{2+} ion. The high stability of UO_2^{2+} complexes of PDA to dissociation in a biological

- (2) Choppin, G. R. *Radiochim. Acta* **1983**, 32, 43.
- (3) Shannon, R. D. *Acta Crystallogr., Sect. A* **1976**, 32, 751.
- (4) Diamond, R. M.; Street, K.; Seaborg, G. T. *J. Am. Chem. Soc.* **1954**, 76, 1461.
- (5) Nash, K. L. In *Handbook on the Physics and Chemistry of Rare Earths*; Gschneider, K. A., Jr., Eyring, L., Choppin, G. R., Lander, G. H., Eds.; North-Holland: Amsterdam; Vol 18, p 197.

- (6) Tian, G.; Zhu, Y.; Xu, J. *Solvent Extr. Ion Exch.* **2001**, 19, 993.
- (7) Petit, L.; Adamo, C.; Maldivi, P. *Inorg. Chem.* **2006**, 45, 8517.
- (8) Morss, L. R.; Rogers, R. D. *Inorg. Chim. Acta* **1997**, 255, 193.
- (9) Melton, D. L.; VanDerveer, D. G.; Hancock, R. D. *Inorg. Chem.* **2006**, 45, 9306.
- (10) Cram, D. J.; Cram, J. M. *Acc. Chem. Res.* **1978**, 11, 49.
- (11) Hancock, R. D. *Acc. Chem. Res.* **1990**, 26, 875.
- (12) Hancock, R. D.; Martell, A. E. *Chem. Rev.* **1989**, 89, 1875.
- (13) Martell, A. E.; Smith, R. M. *Critical Stability Constant Database 46*; National Institute of Science and Technology (NIST): Gaithersburg, MD, 2003.

environment, and their recognition by monoclonal antibodies has been observed.¹⁴ At the same time, the structural chemistry of PDA complexes with larger metal ions has received little attention, being confined to the structure of the Ca(II) complex,⁹ with other reported structures being for small metal ions such as Cu(II) and Ni(II).^{15–19} We thus report here the synthesis and structures of [UO₂(PDA)] (1) and [Th(PDA)₂(H₂O)₂].H₂O (2), which are larger metal ions, as well as the formation constants of PDA with Th⁴⁺. Conventional approaches to obtaining crystalline samples of 1 and 2 yielded only powders, so that we report here successful use of hydrothermal methods²⁰ for their synthesis. The previous determination⁹ of formation constants for PDA also proved challenging because of the very high log *K*₁ values and low protonation constants, and in the end only competition reactions between PDA and EDTA or DTPA yielded log *K*₁ values for PDA. With Th(IV), competition between DTPA and PDA did not provide a viable approach to determining log *K*₁ because complex equilibria involving formation of mixed ligand complexes of PDA and DTPA were observed. We thus report here a different approach involving displacement of PDA from its complexes with Th(IV) by OH[−] ion at high pH to form [Th(OH)₄] solution species, monitored by UV–visible spectroscopy. We also report the interactions of the UO₂²⁺/PDA system with OH[−] as the pH is raised, although we do not here report log *K*₁ for UO₂²⁺/PDA because alternative potentially more accurate approaches are being developed.

Experimental Section

Materials. PDA was synthesized by a literature method.²¹ The metal perchlorates were obtained from VWR or Strem in 99% purity or better and used as received. All solutions were made up in deionized water (Milli-Q, Waters Corp.) of >18 MΩ cm^{−1} resistivity.

Synthesis of [UO₂(PDA)] (1). Commercial UO₂(NO₃)₂·6H₂O (depleted, J. T. Baker Chemical, Co.) was used without further purification. Crystals of [(UO₂)(PDA)] were obtained from a hydrothermal reaction mixture that contained 84 mg (0.167 mmol) of UO₂(NO₃)₂·6H₂O, 53 mg (0.198 mmol) of PDA, and 1.67 g of deionized H₂O (92.5 mmol). These reagents were combined in a 23 mL Teflon-lined stainless steel reaction vessel (initial pH 1.36) and heated to 180 °C for 1 day. The reaction mixture was then allowed to cool to room temperature. The yellow mother liquor

(final pH 1.03) was extracted and the remaining yellow crystals were subsequently washed with both distilled water and ethanol then allowed to air-dry at room temperature. Analysis Calcd for C₁₄H₆N₂O₆U: C, 31.34; H, 1.12; N, 5.22. Found: C, 31.76; H, 1.06; N, 5.35.

Synthesis of [Th(PDA)₂(H₂O)₂].H₂O (2). Th(NO₃)₄·4H₂O was purchased from Strem Chemicals and used without further purification. Crystals of [Th(PDA)₂(H₂O)₂].H₂O were obtained from a hydrothermal reaction mixture that contained 81 mg (0.167 mmol) of Th(NO₃)₄·4H₂O, 44 mg (0.167 mmol) of PDA, and 1.69 g of deionized H₂O (93.6 mmol). These reagents were combined in a 23 mL Teflon-lined stainless steel reaction vessel (initial pH 1.23) and heated to 180 °C for 1 day. The reaction mixture was then allowed to cool to room temperature. The clear colorless mother liquor (final pH 0.95) was extracted and the remaining clear colorless crystals were subsequently washed with both distilled water and ethanol and allowed to air-dry at room temperature. Anal. Calcd for C₂₈H₁₈N₄O₁₁Th: C, 41.08; H, 2.20; N, 6.85. Found: C, 40.46; H, 2.08; N, 6.81.

Structure Determination. The crystal structures of (UO₂)(C₁₄H₆N₂O₄) (1) and Th(C₁₄H₆N₂O₄)₂(H₂O)₂·H₂O (2) were determined via single-crystal X-ray diffraction. A representative crystal of each compound was mounted on a glass fiber using epoxy gel. Intensity data were collected on a Bruker SMART diffractometer equipped with an APEX II CCD detector. Data processing was performed using SAINT.²² The structures were solved using direct methods while the refinement was carried out using SHELXL-97²³ within the WINGX software suite.²⁴ Powder X-ray diffraction data were collected on a Rigaku MiniFlex II Desktop X-ray Diffractometer (Cu Kα, 3–60°, 0.05° step, 1.0 s step^{−1}) and manipulated utilizing the JADE²⁵ software package. The observed and calculated powder diffraction patterns for both 1 and 2 were in excellent agreement. The structures of 1 and 2 are shown in Figures 4 and 5. Details of the structure determinations are given in Table 1, and coordinates for 1 and 2 have been deposited with the Cambridge Structural Database (CSD).²⁶ A selection of bond lengths and angles for 1 and 2 are given in Tables 2 and 3.

Fluorescence Studies. These were conducted on a Shimadzu RF-5301 PC Spectrofluorophotometer (ligand excitation wavelength, 270 nm; uranyl excitation wavelength, 365 nm slit width: 3.0 nm (excitation) and 3.0 nm (emission);²⁷ sensitivity, high with a UV-39 filter.

Formation Constant Determination. These were determined by UV–visible spectroscopy following procedures similar to those of Choppin et al.²⁸ for studying 1,10-phen complexes of Th(IV). UV–visible spectra were recorded using a Varian 300 Cary 1E UV–visible spectrophotometer controlled by Cary Win UV Scan Application, version 02.00(5), software. A VWR symphony SR60IC pH meter with a VWR symphony gel epoxy semimicro combination pH electrode was used for all pH readings, which were made in the external titration cell, with N₂ bubbled through the cell to exclude CO₂. The pH meter was calibrated by titration of 25 mL of 0.01 M HClO₄ in 0.09 M NaClO₄ with 50 mL of 0.01 M NaOH in 0.09 M NaClO₄, covering the pH range from 2 to 12. The standard potential *E*⁰ and Nernstian slope were determined from a least-squares fit of measured potential for the cell versus calculated pH. The cell containing 50 mL of ligand/metal solution was placed in a bath thermostatted to 25.0 ± 0.1 °C, and a peristaltic pump

(14) Blake, R. C.; Pavlov, A. R.; Khosraviani, M.; Emsley, H. E.; Kiefer, G. E.; Yu, H.; Li, X.; Blake, D. A. *Bioconjugate Chem.* **2004**, *15*, 1125.

(15) Moghimi, A.; Alizadeh, R.; Shokrollahi, A.; Aghabozorg, H.; Shamsipur, M.; Shokravi, A. *Inorg. Chem.* **2003**, *42*, 1616.

(16) Xie, Y.-B.; Li, J.-R.; Bu, X.-H. *J. Mol. Struct.* **2005**, *741*, 249.

(17) Park, K. M.; Yoon, I.; Seo, J.; Lee, Y. H.; Lee, S. S. *Acta Crystallogr., Sect. E* **2001**, *57*, m154.

(18) Moghimi, A.; Alizadeh, R.; Aragoni, M. C.; Lippolis, V.; Aghabozorg, H.; Norouzi, P.; Isaia, F.; Sheshmani, S. *Z. Anorg. Allg. Chem.* **2005**, *631*, 1941.

(19) Moghimi, A.; Alizadeh, R.; Aghabozorg, H.; Shokravi, A.; Aragoni, M. C.; Demartin, F.; Isaia, F.; Lippolis, V.; Harrison, A.; Shokrollahi, A.; Shamsipur, M. *J. Mol. Struct.* **2005**, *750*, 166.

(20) (a) Borkowski, L. A.; Cahill, C. L. *Cryst. Growth Des.* **2006**, *6*, 2248.

(b) Borkowski, L. A.; Cahill, C. L. *Cryst. Growth Des.* **2006**, *6*, 2241.

(c) Sheets, W. C.; Mugnier, E.; Barnabe, A.; Marks, T. J.; Poepelmeier, K. R. *Chem. Mater.* **2006**, *18*, 7.

(21) Chandler, C. J.; Deady, L. W.; Reiss, J. A. *J. Heterocycl. Chem.* **1981**, *18*, 599.

(22) SAINT, version 5.053, Area-Detector Integration Software; Siemens Industrial Automation, Inc.: Madison, WI, 1998.

(23) Sheldrick, G. M. *SHELX97, Programs for Crystal Structure Analysis (Release 97–2)*; University of Göttingen: Göttingen, Germany, 1998.

(24) WingX. Farrugia, L. J. *J. Appl. Crystallogr.* **1999**, *32*, 837.

(25) JADE, version 6.1; Materials Data Inc.: Livermore, CA, 2002.

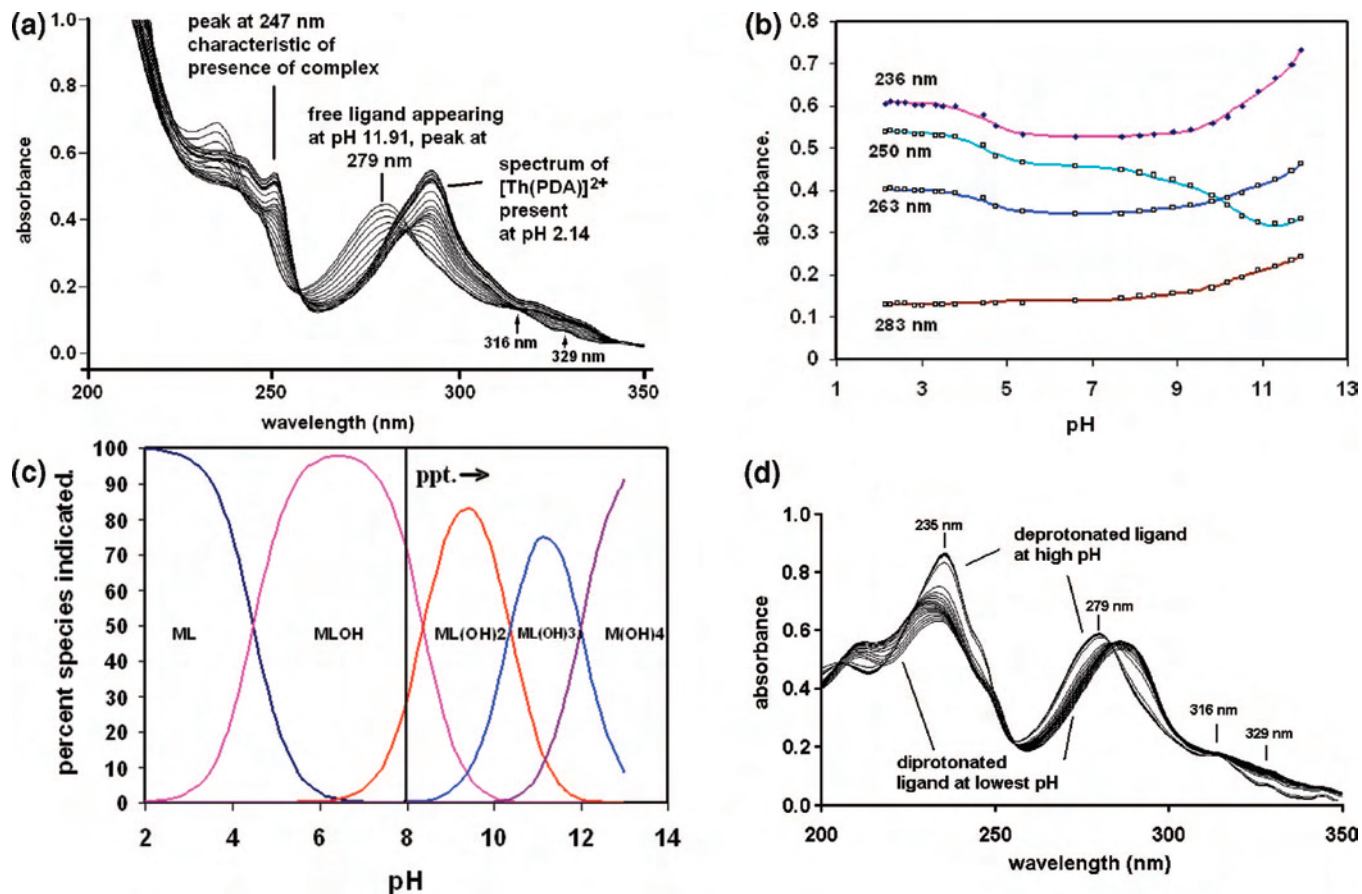
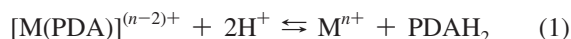


Figure 2. (a) Set of UV spectra of 2.00×10^{-5} M PDA plus 2.00×10^{-5} M Th(IV) in 0.1 M NaClO₄ at 25.0 °C as a function of pH between pH 2.14 and 11.91. The two small peaks indicated at 316 and 329 nm are typical of the fully deprotonated free PDA ligand. (b) Variation of absorbance at different wavelengths as a function of pH for 2.00×10^{-5} M PDA and 2×10^{-5} M Th(IV) in 0.1 M NaClO₄ at 25 °C. The points are the experimental values from panel a, whereas the solid lines are theoretical curves for absorbance vs pH calculated using EXCEL²⁸ as described in the text. (c) Species distribution diagram calculated for 2×10^{-5} M of both Th(IV) and PDA as a function of pH, using formation constants given in Table 4. Abbreviations: M = Th(IV), L = PDA. (d) Spectra of a solution of 2×10^{-5} M PDA in 0.1 M NaClO₄ at 25 °C at a series of pH values from 2.08 to 9.39.

was used to circulate the solution through a 1 cm quartz flow cell situated in the spectrophotometer. The pH was altered in the range 2–12 by additions to the external titration cell of small amounts of HClO₄ or NaOH as required using a micropipette. After each adjustment of pH, the system was allowed to mix by operation of the peristaltic pump for 15 min prior to recording the spectrum. Mixing was further promoted by use of a magnetic stirrer in the external titration cell. Repeat spectra were run periodically for selected titration points after a further half-hour of mixing to ensure that equilibrium was being established in the time allowed for mixing. For the Th(IV) system titrations were performed in duplicate with 2×10^{-5} M each of Th⁴⁺ and PDA, and at 4×10^{-6} M of each of Th⁴⁺ and PDA.

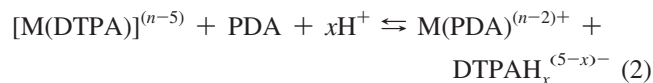
Results and Discussion

Formation Constants. The equilibrium constants determined here are given in Table 4. The most common approach to formation constant determination involves²⁹ competition between the metal ion and protons for the ligand, as in



If the protonation constants are known, then it is a simple matter to calculate $\log K_1$ for the ML complex if the reaction quotient for 1 is determined. For PDA the protonation constants are⁹ rather low at 4.75 and 2.53 (0.1 M NaClO₄

and 25 °C), whereas $\log K_1$ values are very high for a tetradentate ligand, so that only for Mg(II), Ca(II), Sr(II), and Ba(II) was $\log K_1(PDA)$ low enough that 1 would proceed to the right at a pH above 1.0. For other metal ions, competition reactions with the ligands EDTA or DTPA were used (eq 2)⁹



The displacement of DTPA from its complex with the metal ion M by PDA would take place as the pH was lowered because of the much higher protonation constants¹³ of DTPA than PDA. For the metal ions studied here, Th(IV), and UO₂²⁺, competition reactions between PDA and DTPA or EDTA were not suitable for the determination of $\log K_1(PDA)$. For UO₂²⁺, DTPA and EDTA were not able to displace PDA from its complexes at any pH, and even in a 100 fold excess of DTPA, as evidenced by the persistence of the UO₂²⁺ complexes with PDA over the pH range 2–12. Th(IV) in the presence of PDA and DTPA appeared to form a mixed-ligand complex that broke up at higher pH to give free PDA. The evidence that a mixed-ligand complex formed between DTPA and PDA with Th(IV) was that, although

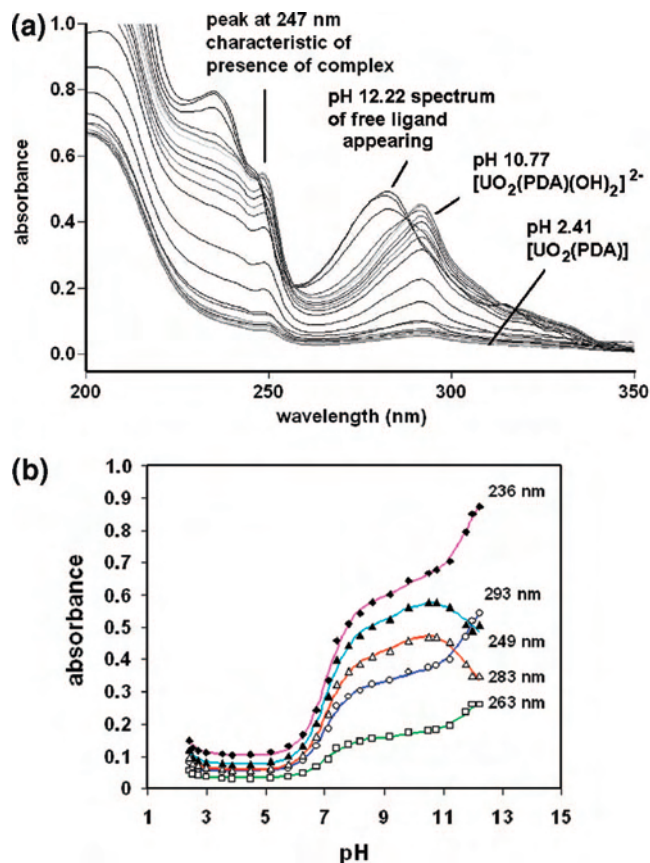


Figure 3. (a) Set of UV spectra of 2.00×10^{-5} M PDA plus 2.00×10^{-5} M UO_2^{2+} in 0.1 M NaClO_4 at 25.0°C as a function of pH between pH 2.41 and 12.22. (b) Variation of absorbance with pH for the UO_2^{2+} /PDA system (both 2.00×10^{-5} M) in 0.1 M NaClO_4 at 25°C . The points are the experimental points, whereas the solid lines are theoretical curves of absorbance versus pH calculated for each wavelength.

Table 1. Crystallographic Data for $[\text{UO}_2(\text{PDA})]$ (1) and $[\text{Th}(\text{PDA})_2(\text{H}_2\text{O})_2] \cdot \text{H}_2\text{O}$ (2)

	1	2
empirical formula	$\text{C}_{14}\text{H}_6\text{N}_2\text{O}_6\text{U}$	$\text{C}_{28}\text{H}_{18}\text{N}_4\text{O}_{11}\text{Th}$
<i>M</i>	536.24	812.46
<i>T</i> (K)	298(2)	298(2)
cryst syst	orthorhombic	triclinic
space group	<i>Pnma</i>	<i>P</i> $\bar{1}$
<i>a</i> (Å)	11.1318(7)	7.6190(15)
<i>b</i> (Å)	6.6926(4)	10.423(2)
<i>c</i> (Å)	17.3114(12)	17.367(4)
α (deg)	90	94.93(3)
β (deg)	90	97.57(3)
γ (deg)	90	109.26(3)
<i>V</i> (Å ³)	1289.71(14)	1278.3(4)
<i>Z</i>	4	2
μ (mm ⁻¹)	12.623	5.909
no. of reflns collected	20119	9412
<i>R</i> _{int} (independent reflns)	0.0972 (1453)	0.1122 (4474)
final <i>R</i> indices [<i>I</i> ≥ 2σ(<i>I</i>)]	0.0313	0.0654
<i>R</i> indices (all data)	0.0654	0.0955

the spectra at low pH were typical of a PDA complex with a large metal ion, the spectra were different from those of the Th(IV)/PDA complex with no DTPA present. In particular, the marked change in absorbance at a pH of about 4.6 when no DTPA was present (Figure 2b) was absent, suggesting that the DTPA was complexing with the Th(IV) in its PDA complex. The complexity of the equilibria involved prevented a straightforward calculation of log

$K_1(\text{PDA})$ for Th(IV) from the results obtained. Instead, for solutions containing Th(IV) and PDA only, as the pH approached 12, it was found that displacement appeared to take place according to eq 3.



Thus, from a knowledge of the log $K_n(\text{OH}^-)$ values¹³ for Th(IV), one should then be able to calculate²⁹ log $K_1(\text{PDA})$ for the complex with Th(IV). It was found that the displacement of the Th(IV) from its PDA complex occurred in distinct steps. In Figure 2a is shown the set of spectra for a 2×10^{-5} M Th(IV)/PDA solution as a function of pH from 2.14 to 11.91. In Figure 2b is shown the variation of absorbance at different wavelengths for the Th(IV)/PDA solution as a function of pH. The points drawn in are experimental values of absorbance, whereas the solid lines are theoretical curves of absorbance versus pH calculated for the constants corresponding to the observed protonation equilibria, and incorporating the fitted extinction coefficients of the L, ML, and ML(OH)_{*n*} species present in solution. The theoretical curves of absorbance versus pH in Figure 2b were fitted to the experimental points using the SOLVER module of the program EXCEL.³⁰ The standard deviations of these protonation constants given in Table 4 were calculated using the SOLVSTAT macro provided with ref 30.

Thorium(IV)/PDA. For the sets of UV spectra of 2×10^{-5} M Th(IV)/PDA in Figure 2a, four protonation equilibria were apparent in the curves of absorbance versus pH shown in Figure 2b. At the last protonation step at pH 12.0, the spectrum of the free ligand becomes apparent, the assignment of which is supported by the two small peaks at 316 and 329 nm (Figure 2a) that are characteristic of the deprotonated PDA dianion. The spectra of the PDA ligand alone between pH 2 and 11 are given in Figure 2d to allow comparison with those in Figure 2a. The initial spectrum at pH 2.14 in Figure 2a is reasonably assigned as that of $[\text{Th}(\text{PDA})]^{2+}$ because it has the sharp band at 247 nm characteristic⁹ of complexation of PDA by large metal ions that fit the “cleff” of PDA well, i.e., have an ionic radius of about 1.0 Å. A reasonable interpretation is that the four protonation equilibria (eqs 4–7) represent the addition of three hydroxides to the Th(IV)/PDA complex, with the final step (eq 7) being the removal of the Th(IV) from the PDA and the formation of $\text{Th}(\text{OH})_4(\text{aq})$ plus the PDA dianion, which is present at pH values above 5 (the pH values indicated are the midpoints for each of the four successive deprotonation equilibria)

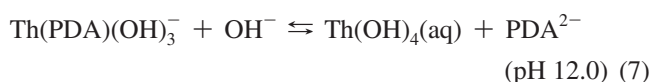
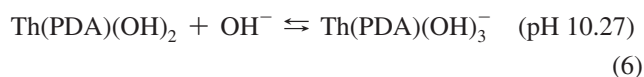
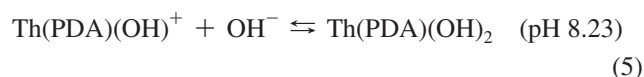


Table 2. Selection of Bond Lengths (Å) and Angles (deg) in [UO₂(PDA)] (1)

U1–O1	1.767(4)	U1–O1'	1.767(4)	U1–O4	2.279(6)
U1–O3'	2.345(6)	U1–O2	2.423(6)	U1–N2	2.543(7)
U1–N1	2.572(7)				
O1–U1–O1'	176.4(3)	O1–U1–O4	91.80(14)	O1–U1–O3	90.54(13)
O4–U1–O3	79.7(2)	O1–U1–O2	88.25(14)	O4–U1–O2	171.6(2)
O3–U1–O2	91.9(2)	O1–U1–N2	90.60(13)	O4–U1–N2	63.8(2)
O3–U1–N2	143.49(19)	O4–U1–N1	125.8(2)	O3–U1–N1	154.5(2)
O2–U1–N1	62.58(19)	N2–U1–N1	62.0(2)		

Table 3. Selection of Bond Lengths (Å) and Angles (deg) in [Th(PDA)₂(H₂O)₂].H₂O (2)

Th1–O5	2.399(10)	Th1–O7	2.405(9)	Th1–O3	2.443(9)
Th1–Ow1	2.473(9)	Th1–O1	2.474(8)	Th1–Ow2	2.532(9)
Th1–N4	2.652(11)	Th1–N3	2.658(12)	Th1–N1	2.718(11)
Th1–N2	2.744(13)				
O5–Th1–O7	152.0(3)	O5–Th1–O3	70.8(3)	O7–Th1–O3	90.3(3)
O5–Th1–Ow1	80.1(3)	O7–Th1–Ow1	74.2(3)	O3–Th1–Ow1	71.4(3)
Ow1–Th1–O1	125.6(3)	O5–Th1–Ow2	70.0(3)	Ow1–Th1–Ow2	147.6(3)
O7–Th1–N4	60.7(4)	Ow1–Th1–N4	68.9(3)	Ow2–Th1–N4	137.3(3)
O5–Th1–N3	60.5(3)	O1–Th1–N3	63.8(3)	N4–Th1–N3	60.1(4)
O1–Th1–N1	59.0(3)	O7–Th1–N2	63.2(3)	O3–Th1–N2	60.4(3)
N3–Th1–N2	178.9(4)	N1–Th1–N2	58.8(3)		

Table 4. Equilibrium Constants Determined or Used Here in the Measurement of the log *K*₁ Values for Th(IV) and UO₂²⁺ with PDA^a

equilibrium	log <i>K</i>	reference
H ⁺ + OH [−] ⇌ H ₂ O	13.78	13
UO ₂ (PDA) + OH [−] ⇌ UO ₂ (PDA)OH [−]	6.72(6)	this work
UO ₂ (PDA)OH [−] + OH [−] ⇌ UO ₂ (PDA)(OH) ₂ ^{2−}	4.25(6)	this work
UO ₂ (PDA) + H ⁺ ⇌ UO ₂ (PDA)H ⁺	1.5(2)	this work
Th(PDA) ²⁺ + OH [−] ⇌ Th(PDA)(OH) ⁺	9.17(4)	this work
Th(PDA)(OH) ⁺ + OH [−] ⇌ Th(PDA)(OH) ₂	5.25(9)	this work
Th(PDA)(OH) ₂ + OH [−] ⇌ Th(PDA)(OH) ₃ [−]	3.51(5)	this work
Th(PDA)(OH) ₃ [−] + OH [−] ⇌ Th(OH) ₄ + PDA ^{2−}	−3.4(2)	this work
Th ⁴⁺ + PDA ^{2−} ⇌ Th(PDA) ²⁺	25.7(9)	this work
Th ⁴⁺ + DTPA ^{5−} ⇌ Th(DTPA) [−]	28.7(1)	13
Th ⁴⁺ + OH [−] ⇌ Th(OH) ³⁺	10.0	13
Th(OH) ³⁺ + OH [−] ⇌ Th(OH) ₂ ²⁺	9.6	13
Th(OH) ₂ ²⁺ + OH [−] ⇌ Th(OH) ₃ ⁺	10.7	13
Th(OH) ₃ ⁺ + OH [−] ⇌ Th(OH) ₄ (aq)	9.9	13
2 Th ⁴⁺ + 2 OH [−] ⇌ Th ₂ (OH) ₂ ⁶⁺	22.4	13
4 Th ⁴⁺ + 8 OH [−] ⇌ Th ₄ (OH) ₈ ⁸⁺	91.2	13
Th(OH) ₄ (s) ⇌ Th ⁴⁺ + 4 OH [−]	−50.7	13

^a In 0.1 M NaClO₄ at 25 °C.

One can be reasonably sure that the first three equilibria represent monomeric species in solution because the constants are independent of overall complex concentration. Thus, the hydrolysis constants obtained with 2×10^{-5} M Th(IV)/PDA are the same as those obtained with 4×10^{-6} M Th(IV)/PDA. If dimers such as [Th₂(PDA)₂(OH)₂]²⁺ were being formed rather than the postulated monomer in equilibrium 4 above, then the hydrolysis would occur at a higher pH for the 4×10^{-6} M solution than the 2×10^{-5} M solution.

These four constants can be combined with log β₄ = 40.2 for Th(OH)₄(aq)¹³ to give log *K*₁(PDA) = 25.7 for Th(IV). As an aid to visualizing the species present in solution, a species distribution diagram for the 2×10^{-5} M Th(IV)/PDA system is shown in Figure 2c. The above value of log β₄ for Th(OH)₄ was reported¹³ at ionic strength 3.0, so that log *K*₁(PDA) for Th(IV) might be revised somewhat should a corroborated and generally agreed upon value of log β₄ for Th(OH)₄ at ionic strength 0.1 become available (see discussion below of problems of the correct value for log β₄ for Th(OH)₄). What is important here is that log *K*₁(PDA) for Th(IV) is very large. The stabilization of the PDA complex of Th(IV) relative to its less preorganized analog EDDA is (Table 5) on the order of 12 log units. This massive

stabilization can be compared with 8 log units for the similarly sized trivalent Gd(III) and 3.3 log units for the divalent Ca(II). The origin of the increasing stabilization of complexes of PDA with increasing metal ion charge has been discussed.⁹ For metal ions of higher charge, such as the trivalent Bi(III) or In(III) ions, affinity for aromatic N-donor ligands such as 1,10-phen or TPEN is relatively low,³² as compared to their affinity for saturated N-donor ligands. One notes the low affinity of Th(IV) for 1,10-phen,²⁸ with log *K*₁ = 2.0, with a remarkable increase of some 24 log units in passing to log *K*₁ for the PDA complex, produced by simply adding two acetate groups to 1,10-phen to give PDA. It seems probable that this stabilization is due to the greater need for metal ions of higher charge to stabilize the complexes they form by H-bonding with the solvent. Aromatic N-donors such as are present on 1,10-phen or TPEN are not able to H-bond with the solvent, and so their complexes with trivalent or tetravalent metal ions are considerably destabilized.³² This effect is much smaller for divalent metal ions such as Cu(II) or Pb(II), so that the relative stability of their complexes with aromatic N-donors is quite high. However, a ligand such as PDA has a synergistic combination of donor groups, in that the charged carboxylate groups fulfill the function of lowering the charge on the metal ion, thus enabling the bonding strength of the pyridyl donor groups to become apparent. It should be noted that in the gas-phase pyridine is^{12,33,34} a stronger proton base than ammonia, but that in water pyridine is a weaker base because of the lesser ability of the pyridinium cation to H-bond with the solvent. In PDA, the greater intrinsic basicity of the pyridyl group becomes manifest with its

(26) Allen, F. H. *Acta Crystallogr., Sect. B* **2002**, *58*, 380; Cambridge Structure Database, version 1.9, 2006.

(27) Almond, P. M.; Talley, C. E.; Bean, A. C.; Peper, S. M.; Albrecht-Schmitt, T. E. *J. Solid State Chem.* **2000**, *154*, 635–41.

(28) Xia, Y. X.; Chen, J. F.; Choppin, G. R. *Talanta* **1996**, *43*, 2073.

(29) Martell, A. E.; Motekaitis, R. J. *The Determination and Use of Stability Constants*; VCH Publishers: New York, 1989.

(30) Billo, E. J. *EXCEL for Chemists*; Wiley-VCH: New York, 2001.

(31) ORTEP-3 for Windows, version 1.08. Farrugia, L. J. *J. Appl. Crystallogr.* **1997**, *30*, 565.

(32) Harrington, J. M.; Oscarson, K. A.; Jones, S. B.; Bartolotti, L. J.; Hancock, R. D. *Z. Naturforsch. B* **2007**, *62b*, 386.

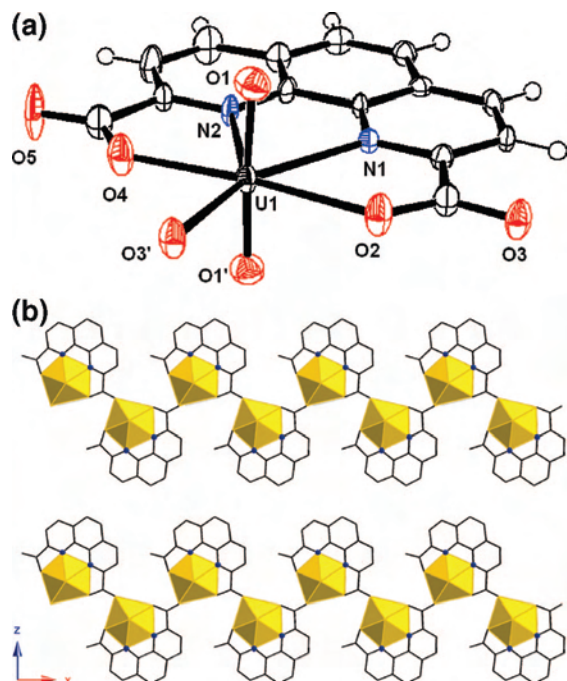


Figure 4. (a) ORTEP³¹ drawing of the complex [UO₂(PDA)] (1)/ Ellipsoids are shown at the 50% probability level. Symmetry equivalents: (i) $x, -y + 1/2, z$; (ii) $x + 1/2, -y + 1/2, -z + 1/2$. The atom O(3)' is a bridging carboxylate oxygen from a neighboring UO₂/PDA individual. (b) A view of [UO₂(PDA)] down the [010] direction. The polyhedra are the uranium pentagonal bipyramids whereas the black lines are PDA ligands. The spheres are the nitrogen atoms from the PDA. The hydrogen atoms have been omitted for clarity. This sheet of [UO₂(PDA)] complexes π -stacks on similar sheets above and below it.

combination with the two acetate groups that reduce the charge on Th(IV). One predicts that the affinity of PDA for Pu(IV), the most stable oxidation state of Pu, should be even higher than found for Th(IV), which may lead to useful applications of PDA-type ligands in complexing Pu. Pu(IV) has an ionic radius³ of 0.86 Å, which is quite large, and Pu(IV) is a considerably stronger Lewis acid than Th(IV) (compare $\log K_1(\text{OH}^-) = 13.5$ for Pu(IV) versus 10.0 for Th(IV)¹³), which should lead to remarkable affinity for PDA. How well Pu(IV) might fit PDA is shown by six structures²⁶ of Pu(IV) complexes where Pu–O averages 2.41 Å, as compared to the average Th–O of 2.43 Å found in **2** below. Because of its great affinity for metal ions of higher charge, PDA should also be able to stabilize higher oxidation states such as Am(IV), thus greatly enhancing the ability to separate Am from Ln(III) cations.

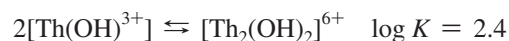
A reviewer has pointed out the great tendency of highly charged metal ions such as Th(IV) to form polymeric hydroxy species¹³ in aqueous solution. A considerable number of $\log K$ values relating to the formation of such dimeric and polymeric hydroxyl species for Th(IV) are found in the compilation of Smith and Martell,¹³ two of which, for the formation of [Th₂(OH)₂]⁶⁺ and [Th₄(OH)₈]⁸⁺, are included in Table 4 as representative examples. As suggested as a possibility by the reviewer, at the low total metal ion

Table 5. Comparison of $\log K_1(\text{PDA})$ and $\log K_1(\text{EDDA})$ Values Illustrating the Effect of Metal Ion Size and Charge on the Stabilization of PDA Relative to EDDA Complexes^a

	ionic radius (Å)	$\log K_1(\text{PDA})$	$\log K_1(\text{EDDA})$	difference in $\log K_1$
Ba ²⁺	1.36	5.4	3.3	2.1
Pb ²⁺	1.19	11.4	10.6	0.8
Sr ²⁺	1.18	5.6	3.6	2.0
Ca ²⁺	1.00	7.3	4.0	3.3
La ³⁺	1.03	13.5	7.0	6.5
Gd ³⁺	0.93	16.1	8.1	8.0
Th ⁴⁺	0.94	25.7	(13.9) ^b	~12
Cd ²⁺	0.95	12.8	9.1	3.7
Mg ²⁺	0.74	3.5	4.0	-0.5
Zn ²⁺	0.74	11.0	11.1	-0.1
Cu ²⁺	0.57	12.8	16.2	-3.4

^a For ligand abbreviations, see Figure 1. $\log K_1$ values at 25 °C, ionic strength 0.1. $\log K_1(\text{PDA})$ values from ref 9 or else this work (Th(IV) and UO₂²⁺), $\log K_1(\text{EDDA})$ values ref 13. ^b Estimated from $\log K = 6.5$ ³⁹ for Th⁴⁺ + LH⁻ \rightleftharpoons ThLH³⁺ (L = EDDA) by combining with a typical value¹³ of $\log K = 2.2$ for ML + H⁺ \rightleftharpoons MLH⁺ for aminocarboxylate ligands.

concentrations used here, such species may not actually form to any significant extent. This can be understood by representing the formation of these species as polymerization equilibria



One sees that with total Th(IV) of 2×10^{-5} M, or even more so, 4×10^{-6} M, none of these polymeric species will form. In line with this, the fact that the equilibria involving formation of [Th(PDA)(OH)_{*n*}]^{(2-*n*)+} species in eqs 4–7 occur at the same pH values at both 2×10^{-5} M and 4×10^{-6} M overall complex concentration means that these [Th(PDA)(OH)_{*n*}]^{(2-*n*)+} species are monomeric. A further factor reducing the possibility of formation of polymeric Th(IV) hydroxyl complexes in the solutions studied here is that in the presence of PDA the actual free Th(IV) is well below the total Th(IV) present. At pH 6, for example, the concentration of the dominant solution species not complexed by PDA, which is [Th(OH)₄](aq), is calculated for Figure 2c to be 3×10^{-7} M. A reviewer has raised the valid question of whether Th(OH)₄(s) is formed as a precipitate at the higher pH values. With the solubility product K_{so} for Th(OH)₄ of¹³ $1 \times 10^{-50.7}$, calculation of a species distribution diagram as a function of pH (Figure 2(c)) shows that precipitation of Th(OH)₄(s) should occur in the 2×10^{-5} M Th(IV)/PDA system by pH 8. From a thermodynamic point of view, one should thus have Th(OH)₄(s) present in these titrations above pH 8. One can be reasonably certain that this is not the case, because formation of precipitates produces a characteristic rising baseline, and frequently characteristic broad peaks due to the presence of colloidal particulates in the solution. That the spectra for the Th(IV)/PDA system in Figure 2a show none of these characteristics, and that isosbestic points persist up to the final pH of 11.91, is good evidence that no significant quantities of Th(OH)₄(s) particulates are present. This is a phenomenon that has been observed previously³⁵ for Bi(III) metal ion solutions down in the 1×10^{-5} M to

(33) Munson, M. S. B. *J. Am. Chem. Soc.* **1965**, *87*, 2332.

(34) Taft, R. W.; Wolf, J. F.; Beauchamp, J. L.; Scorrano, G.; Arnett, E. M. *J. Am. Chem. Soc.* **1978**, *100*, 1240.

(39) Kinard, W. F.; Grant, P. M.; Baisden, P. A. *Polyhedron* **1989**, *8*, 2385.

(35) Hancock, R. D.; Cukrowski, I.; Mashishi, J. *J. Chem. Soc., Dalton Trans.* **1993**, 2895.

10^{-6} M range, i.e., that thermodynamically one expects precipitates of the metal hydroxide to form, but kinetically precipitate formation is so slow at the low metal ion concentrations used that precipitates do not form during the time of the titration. A further point raised by a reviewer is the high accuracy claimed for the hydrolysis constants in Table 4, in view of the low accuracy of the final $\log K_1(\text{PDA})$ value for Th(IV). These hydrolysis constants, represented by eqs 7, do not depend on the value of $\log K_1(\text{PDA})$, and in fact, the latter is calculated from the hydrolysis constants.

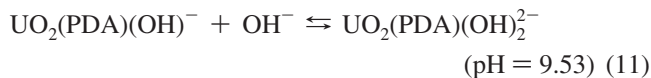
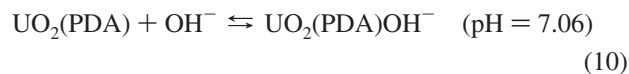
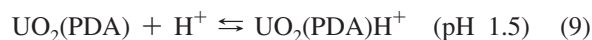
As mentioned by a reviewer, a problem with the approach adopted in determining $\log K_1(\text{PDA})$ for Th(IV) in this paper arises from the uncertainty in the value for $\log \beta_4(\text{OH}^-)$ for Th(IV), even though Smith and Martell cite¹³ some 35 papers on the question. Experimental values of $\log \beta_4(\text{OH}^-)$ for Th(IV) range³⁶ from 39.0 ± 0.5 in 1.0 M NaClO₄³⁷ to 42.58 ± 0.08 in 0.1 M NaClO₄.³⁸ The difficulty in determining an accurate value for $\log \beta_4(\text{OH}^-)$ for Th(IV) arises³⁶ from the typical slow kinetics involved in hydrolysis of metal ions, and the presence of colloidal precipitates that affect the calculated value of $\log \beta_4(\text{OH}^-)$. The value of $\log K_1(\text{PDA})$ for Th(IV) in the titrations reported here relates to $\log \beta_4(\text{OH}^-)$ for Th(IV) as follows

$$\log K_1(\text{PDA}) = \log \beta_4(\text{OH}^-) - (9.17 + 5.25 + 3.51 - 3.4) \quad (8)$$

where 9.17 through -3.4 are the $\log K$ values for the hydrolysis of the Th(IV)/PDA complex given in Table 4. Should widely accepted values of $\log \beta_4(\text{OH}^-)$ for Th(IV) at ionic strength 0.1 become available, an improved value of $\log K_1(\text{PDA})$ for Th(IV) can thus be calculated from eq 8. A further point raised by a reviewer is the question of the reproducibility of the titrations carried out here, which is particularly relevant in view of the great difficulties³⁶ experienced in studying hydrolysis reactions of highly acidic metal ions. The hydrolytic equilibria studied for the Th(IV)/PDA complex are reasonably reproducible, with fitted pK values for repeat identical titrations at 2×10^{-5} M complex agreeing to within 0.06 log units. The pK values represented by equations 4–7 given in Table 4 represent simultaneous refinement of both titrations, with the standard deviations being those for the combined titrations. The goodness of fit parameter, R^2 , for the overall fit to the data was 0.9997.

Uranyl/PDA. For the sets of 2×10^{-5} M UO₂²⁺/PDA between pH 2.41 and 12.22 in Figure 3a, three pH-dependent equilibria are apparent, as seen in Figure 3b, where theoretical curves of absorbance versus pH have been fitted to the experimental points. Again, the spectrum of the PDA dianion becomes apparent only at the highest pH, while spectra at lower pH have the sharp small band at 247 nm typical of PDA metal–ligand complexes. The three successive pH-dependent equilibria, plus an additional equilibrium barely

apparent at about pH 2, can be ascribed as (eqs 9–11)



One could calculate $\log K_1(\text{PDA})$ from these equilibria, but Smith and Martell¹³ in their compilation do not regard any of the reported constants for the formation of the [UO₂(OH)₃]⁻ species as reliable, which is needed for the calculation of $\log K_1$. A calculation of $\log K_1(\text{PDA})$ for UO₂²⁺ is therefore not reported here. The present authors are in fact determining $\log K_1(\text{PDA})$ for UO₂²⁺ by means of a competition reaction with Lu³⁺, the results of which will be reported in a future publication. One notes here that the equilibria 9–11 above, combined with less-than-reliable $\log K$ values for the formation of [UO₂(OH)₃]⁻, suggest $\log K_1(\text{PDA}) > 13$ for UO₂²⁺. No ionic radius is available³ for an irregular-shaped cation such as UO₂²⁺, but one may estimate its apparent size by comparing in-plane U–O bond lengths for UO₂²⁺ complexes in the CSD²⁶ with those of Ca²⁺ and Th⁴⁺. What this search yields is UO₂²⁺ (372 structures) U–O in-plane = 2.44 ± 0.11 Å, Ca–O = (302 structures) 2.47 ± 0.10 Å, and Th–O (78 structures) = 2.48 ± 0.10 Å. This suggests that the in-plane bond lengths of UO₂²⁺ are quite close in size to those of Ca²⁺ and Th⁴⁺, and that UO₂²⁺ might be regarded as having an ionic radius referring only to the in-plane bond lengths of roughly 0.95 Å. It thus seems that the UO₂²⁺ ion should fit rather well into the ‘cleft’ of PDA. The value $\log K_1 > 13$ for UO₂²⁺ with PDA is very large for a UO₂²⁺ complex,¹³ compared to $\log K_1(\text{EDTA})$ for UO₂²⁺ of only 9.7. The $\log K_1(\text{PDA}) > 13$ for UO₂²⁺ is exceeded¹³ for simple ligands only by phenolates such as catechol (1,2-dihydroxybenzene), which have $\log K_1 = 15.5$. However, if the very high protonation constants¹³ of catechol (13.3 and 9.3) are factored in, PDA, is a more effective ligand at pH values below 10. The highly preorganized calixarenes of Shinkai et al.⁴⁰ with six acetate donors have higher $\log K_1$ values with UO₂²⁺ of 19.2, but it is not clear that such complex ligands would be economically attractive, although interest in such ligands is still strong.^{41–47}

An unusual feature of the spectra of the [UO₂(PDA)(OH)_n]ⁿ⁻ complexes in Figure 3a is the very weak absorption

(36) Wickleder, M. S.; Fourest, B.; Dorhout, P. K. In *The Chemistry of the Actinide and Transactinide Elements*, 3rd ed.; Morss, L. R., Edelstein, N. M., Fuger, J., Eds.; Springer: Dordrecht, The Netherlands, 2006; Vol. 1, p 119.

(37) Ekberg, C.; Albinsson, Y. *J. Solution Chem.* **2000**, *29*, 63.

(38) Moon, H. C. *Bull. Korean Chem. Soc.* **1989**, *10*, 270.

(40) Shinkai, S.; Koreishi, H.; Ueda, K.; Arimura, T.; Manabe, O. *J. Am. Chem. Soc.* **1987**, *109*, 6371.

(41) Boulet, B.; Bouvier-Capely, C.; Cossonnet, C.; Cote, G. *Solvent Extr. Ion Exch.* **2006**, *24*, 319.

(42) Ten'kovtsev, A. V.; Abramova, L. V.; Dudkina, M. M. *Russ. J. Appl. Chem.* **2006**, *79*, 1494.

(43) Souane, R.; Hubscher, V.; Asfari, Z.; Arnaud, F.; Vicens, J. *Tetrahedron Lett.* **2003**, *44*, 9061.

(44) Kim, J.-H.; Park, J.-H.; Xuan, G.; Kang, S. *Chem. Sens.* **2001**, *17B*, 72.

(45) Sonoda, M.; Nishida, M.; Ishii, D.; Yoshida, I. *Anal. Sci.* **1999**, *15*, 1207.

(46) Beer, P. D.; Drew, M. G. B.; Heseck, D.; Kan, M.; Nicholson, G.; Schmitt, P.; Sheen, P. D.; Williams, G. *J. Chem. Soc., Dalton Trans.* **1998**, *17*, 2783.

(47) Harrowfield, J. *Gazz. Chim. Ital.* **1998**, *127*, 663.

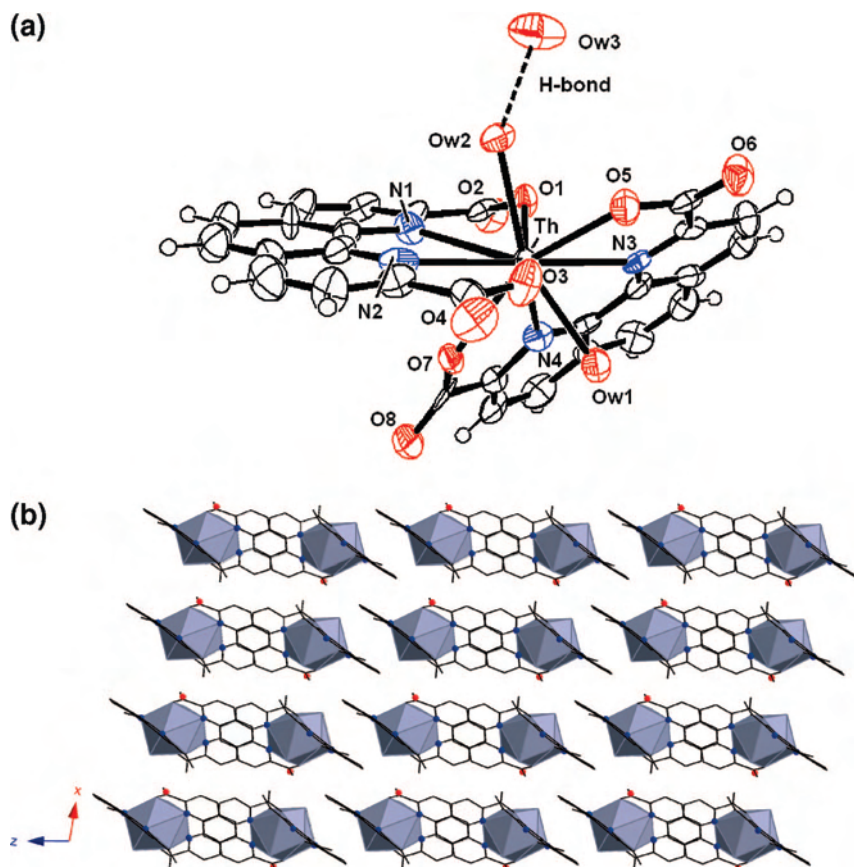


Figure 5. (a) ORTEP³¹ drawing of the complex $[\text{Th}(\text{PDA})_2(\text{H}_2\text{O})_2]\cdot\text{H}_2\text{O}$ (**2**), with thermal ellipsoids shown at the 50% probability level. The structure shows for the PDA ligand to the right how the PDA ligands are bowed, and how the Th atom lies out of the plane of the bowed PDA ligands. Ow1 and Ow2 are waters coordinated to the Th, and Ow3 is a lattice water H-bonded to Ow2. (b) A view of $[\text{Th}(\text{PDA})_2(\text{H}_2\text{O})_2]\cdot\text{H}_2\text{O}$ (**2**) down the [010] direction. The polyhedra are the thorium metal centers, whereas the black lines are the PDA ligands. The spheres are the nitrogen atoms from the PDA. The red spheres are the unbound water molecules. Hydrogen atoms have been omitted for clarity. The diagram shows the π -stacking that typically is involved in the packing of complexes of this type in the unit cell. Some π -stacking is taking place between pairs of PDA ligands almost in the plane of the page (the PDA ligands shown face-on), whereas the other π -stacking is at right angles to the plane of the page (PDA ligands shown edge-on).

Table 6. Bond Lengths and Angles Involving the Coordination around U in $[\text{UO}_2(\text{PDA})]$ (**1**), Compared with the Corresponding Structural Features in the Complexes of UO_2^{2+} with the Much Less Sterically Demanding Phen and Picolinate-Type Ligands Found in the CSD²⁶

	U–O (Å)	N–U–O (deg)	U–O–C (deg)	U–N (Å)	N–U–N (deg)	U–N–C (deg)
structural features of 1 ($[\text{UO}_2(\text{PDA})]$)	2.36	62.9	128.9	2.56	62.62	122.3
corresponding values in $\text{UO}_2/1,10\text{-phen}$ complexes ²⁶				2.60(3)	62.4(7)	120.4(9)
corresponding values in $\text{UO}_2/\text{picolinate}$ type complexes ²⁶	2.41(5)	62.2(1.7)	128.5(1.4)	2.58(5)		

by that at lowest pH, which is thought to be the $[\text{UO}_2(\text{PDA})]$ complex itself. The behavior of the Th(IV)/PDA complexes in Figure 2a is quite typical for⁹ other metal ions such as Gd(III) or Pb(II), without such a weak spectrum for the $[\text{M}(\text{PDA})]$ complex with no hydroxides attached. The experiment was repeated carefully with fresh solutions, and an identical set of spectra was obtained. As discussed below, the weak absorption by the $[\text{UO}_2(\text{PDA})]$ complex may account for its weak fluorescence.

Structure of $[\text{UO}_2(\text{PDA})]$ (1**).** The structure of **1** is seen in Figure 4(a), and a selection of bond angles and lengths for **1** are given in Table 2. The structure of **1** consists of a central uranium (VI) metal center bound to two symmetry-equivalent oxygen atoms, O1, at a distance of 1.767(4) Å resulting in an O1–U1–O1 angle of 176.4(3)° to form the familiar uranyl cation (UO_2^{2+}). One PDA anion is bound to the uranyl cation in a tetradentate fashion through both nitrogen atoms at an average distance of 2.558 Å and through two carboxylate oxygen atoms at an average distance of

2.351 Å. Completing the pentagonal bipyramidal local geometry of the uranium metal centers, an additional carboxylate oxygen atom, O3', from a second PDA anion is bound at a distance of 2.345(6) Å resulting in one-dimensional chains as can be viewed down [010] (Figure 4b). The question of interest here is the evidence that the structure provides on whether the PDA is coordinated to the uranyl group in a low-strain fashion, and what bearing this might have on the slightly lower than expected $\log K_1(\text{PDA})$ suggested here for the UO_2^{2+} cation. The PDA ligand in **1** is almost exactly planar, with the U atom lying in the plane of the ligand, as was also found for the Ca(II)/PDA complex,⁹ which suggests that it is coordinated to the uranyl group in a fairly low-strain manner. Complexes of UO_2^{2+} with simple bidentate ligands such as 1,10-phen and picolinic acid (2-carboxypyridine) should have more nearly ideal geometry involving the donor atoms and the U atom than is true for the more sterically demanding tetradentate PDA ligand. A search of the CSD²⁶ shows 5 structures of uranyl 1,10-phen

complexes, and 13 structures of uranyl complexes with picolinate-type ligands. A comparison of bond angles and lengths involving the UO_2 group and the N and O donors shows that the structural features in **1** are effectively identical to the corresponding structural features in the 1,10-phen and picolinate complexes, and that the coordination of UO_2^{2+} in its PDA complex is probably quite low-strain. This is summarized in Table 6, which shows that the structural features of **1** are very similar to the corresponding structural features in the UO_2^{2+} complexes of phen and picolinic acids, and that the more preorganized structure of the PDA ligand imposes no more steric penalties on its UO_2^{2+} complex than do the sterically much less demanding phen and picolinate ligands.

Structure of $[\text{Th}(\text{PDA})_2(\text{H}_2\text{O})_2]\cdot\text{H}_2\text{O}$ (2**).** The structure of **2** is seen in Figure 5a, and a selection of bond angles and lengths for **2** are given in Table 3. The structure of **2** consists of a central Th(IV) metal center coordinated to two distinct PDA anions, each bound in a tetradentate fashion. Each PDA is bound to the Th(IV) through both nitrogen atoms along with two carboxylate oxygen atoms at an average distance of $\text{Th}-\text{N} = 2.694$ and $\text{Th}-\text{O} = 2.430$ Å. Completing the 10-coordinate local geometry, two water molecules are additionally bound to the Th metal centers at distances of 2.473 and 2.532 Å to create the corresponding $\text{Ow}(1)-\text{Th}(1)-\text{Ow}(2)$ angle of $147.6(3)^\circ$. Around each molecular unit, there is one unbound water molecule, $\text{Ow}(3)$, located 2.751 Å away from $\text{Ow}(2)$. In contrast to the structure of **1**, the PDA ligands in **2** are not planar, but are bowed, and the Th atom lies well out of the plane of the PDA ligands, as shown in Figure 5a. It can be shown using MM (molecular mechanics)⁴⁸ calculations that this distortion of the PDA ligands is brought about by steric crowding. If the two water molecules coordinated to the Th in **2** are removed, and MM calculations are used to generate a structure for $[\text{Th}(\text{PDA})_2]$, completely planar PDA ligands result. If the water molecules are replaced on the Th to give $[\text{Th}(\text{PDA})_2(\text{H}_2\text{O})_2]$, the bowing of the PDA ligands is restored in the MM energy-minimized structure. Inspection of the structure shows that each coordinated water molecule presses on the center of the adjacent PDA ligand, causing it to bow. Work in progress on other ligands related to PDA has shown that bowing and other distortions toward nonplanarity of the ligand are quite common, and do not seem to be accompanied by any major loss in complex stability.

Both structures **1** and **2** involve extensive π -stacking holding layers of the complexes together. In **1**, chains of $[\text{UO}_2(\text{PDA})]$ complexes are held together by bridging carboxylates and form sheets as seen in Figure 4b that π -stack on similar sheets above and below them. In **2**, the two PDA ligands coordinated to each Th do not lie in the same plane, and so (Figure 5b) the π -stacking alternates between pairs of PDA ligands that lie at approximately right angles to the 010 direction of the crystal and those that lie in the 010 direction.

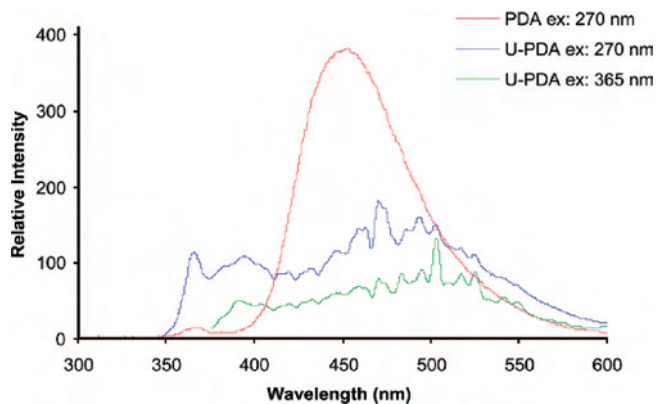


Figure 6. Fluorescence spectra of the PDA ligand and the uranyl PDA complex excited at 279 and 365 nm.

Fluorescence Studies. The fluorescence of uranium(VI) compounds in both the solution and solid state has been known for more than 150 years with the corresponding spectrum resulting from vibronic transitions⁴⁹ of the molecular uranyl cation, $[\text{O}=\text{U}=\text{O}]^{2+}$. As such, fluorescence investigations were conducted on the U-PDA compound in the solid state at room temperature. When the uranyl ion is directly excited at 365 nm⁵⁰ the resulting emission generates only a weak spectrum devoid of the characteristic vibronic fine structure seen in many other compounds.^{51,52} Exploration of sensitized emission with ligand excitation wavelength of 270 nm yields similar results (Figure 6). The observed spectrum is therefore believed to represent the fine structure of the PDA ligand itself and excitation at 365 nm gives rise to the subsequent uranyl emission being reabsorbed as a suggested metal to ligand charge transfer (MLCT).

Conclusions

(1) The expectation⁵³ that a large metal ion of higher charge such as Th(IV) would show remarkably high stability of its PDA complex, particularly as compared to its EDDA complex, is borne out by this study. (2) The UO_2^{2+} complex of PDA possibly shows a modest stabilization as compared to its EDDA complex and may be behaving as expected for a larger divalent metal ion. (3) The structure of the UO_2^{2+} complex of PDA suggests that the fit of the UO_2^{2+} into the cleft of PDA is accompanied by very little steric strain. In contrast, the two PDA ligands coordinated to Th(IV) in $[\text{Th}(\text{PDA})_2(\text{H}_2\text{O})_2]$ are somewhat distorted, which is shown by MM calculation to be due to steric crowding caused by the two water molecules coordinated to Th(IV). It does not appear that such bowing of the PDA leads to significant destabilization of the complex. (4) The combination in PDA of pyridyl donor groups, which normally are poor at reducing the charge

(48) Hyperchem program, version 7.5, Hypercube, Inc., 419 Philip Street, Waterloo, Ontario, N2L 3 × 2, Canada.

(49) Rabinowitch, E.; Belford, R. L. *Spectroscopy and Photochemistry of Uranyl Compounds*; Wiley: New York, 1964.

(50) Almond, P. M.; Talley, C. E.; Bean, A. C.; Peper, S. M.; Albrecht-Schmitt, T. E. *J. Solid State Chem.* **2000**, *154*, 635.

(51) Frisch, M.; Cahill, C. L. *Dalton Trans.* **2006**, 4679.

(52) Frisch, M.; Cahill, C. L. *Dalton Trans.* **2005**, 1518.

(53) Hancock, R. D.; Melton, D. L.; Harrington, J. M.; McDonald, F. C.; Gephart, R. T.; Boone, L. L.; Jones, S. B.; Dean, N. E.; Whitehead, J. R.; Cockrell, G. M. *Coord. Chem. Rev.* **2007**, *251*, 1678.

on metal ions of higher charge such as Th(IV), with carboxylates that reduce the charge on such metal ions, may account for the remarkable affinity of PDA for metal ions of higher charge.

Acknowledgment. The authors thank the National Science Foundation (Grant CHE 0111131) and the University of

North Carolina–Wilmington for generous support for this work.

Supporting Information Available: Crystallographic information in CIF format. This material is available free of charge via the Internet at <http://pubs.acs.org>.

IC701574J